Elastic constants and stability of bcc In-Tl alloys

M. R. Madhava and G. A. Saunders

School of Physics, Bath University, Claverton Down, Bath, BA2 7AY, England

(Received 17 August 1977)

Large single crystals have been grown of the bcc In-Tl alloys which correspond to solid solutions of In in the β (bcc) polymorph of Tl. The components of the elastic-stiffness tensor have been obtained for the alloy compositions 76.5- and 81.5-at.% Tl from ultrasonic-wave velocity measurements made by the pulse-superposition technique. The shear-anisotropy factor $A[=2C_{44}/(C_{11}-C_{12})]$ is found to be large, in agreement with Zener's prediction that $(C_{11}-C_{12})$ should be small in comparison with C_{44} for a bcc material comprised of closed ion shells. A linear extrapolation of the elastic constants of the alloys to vanishing solute concentration has been used to estimate the elastic constants of β-Tl itself. Thus the elastic constants are now available for all the three polymorphs [α(fcc), β(bcc), and ϵ(hcp)] of Tl. Since the elastic constants of the fcc and bcc polymorphs can only be obtained by exptrapolation of alloy data optimized-model-potential calculations have also been made for each polymorph to examine further the validity of the results. Zener has suggested that the stability of the bcc structure found at high temperature for many metals is due to a comparatively large vibrational entropy contribution. To put this hypothesis to the test, the excess entropy ΔS of the bcc phase over the hcp phase has been calculated in the Debye approximation. Results indicate that the stability of the bcc phase of Tl is due to the lower Debye temperature and consequently greater entropy than that of the hcp form.

I. INTRODUCTION

Many metals, Tl among them, undergo a phase transformation from a low-temperature close-packed form to a high-temperature bcc structure. Zener[1-3] has argued that at high temperatures the bcc structure is stable relative to the low-temperature structure because of the relatively large vibrational entropy associated with the accompanying small value of the shear modulus $\frac{1}{2}(C_{11}-C_{12})$. When the bcc phase is stable only well above room temperature (which is the usual case, the alkali metals being exceptions) experimental evidence for structure dependence of the elastic constants or of the lattice vibration spectrum is hard to obtain; at present, sufficient data with which to put Zener's predictions fully to the test are not available for any pure metal. Grimvall and Ebbsjö[4] have recently collected together the somewhat indirect evidence that does exist for certain transition-metal alloys and find it to be in accord with Zener's ideas. Although it is not possible to quench in the bcc form of Tl at room temperature, alloying with In does stabilize the bcc structure and we have been able to grow single crystals of bcc, Tl-rich In-Tl alloys. The elastic constants measured by ultrasonic techniques are used to examine Zener's predictions that $\frac{1}{2}(C_{11}-C_{12})$ should be small for a bcc material comprised of closed-shell ions and that this polymorph is stabilized by a large vibrational-entropy contribution from $\{110\}\langle1\bar{1}0\rangle$ modes to the free energy at high temperatures.

Tl exhibits each of the three most common

structures of the elemental metals: hcp, fcc, and bcc. Reference to the pressure-temperature diagram[5] shows that the stability limits of these three polymorphs can be listed as (i) hcp (ϵ) phase—at mospheric pressure and up to 507 °K; (ii) bcc (β) phase—atmospheric pressure and between 507 °K and the melting point 577 °K; (iii) fcc (α) phase—at room temperature and above 37 kbar: this form is stable only under high pressures. The bcc polymorph cannot be retained at room temperature even using fast-quenching techniques.[6] Yet comparison between the elastic constants is prerequisite for assessing the relative stability of each of the three phases. To do this, recourse has to be made to extrapolation of elastic-constant data obtained for Tl-rich alloys. Previously, estimates of the elastic constants of fcc Tl have been made by extrapolation of data both for fcc In-Tl alloys[7] and for fcc Pb-Tl alloys.[8] The present work provides the first estimate of the elastic constants of bcc Tl. The elastic constants of the normally occurring hcp form have been reported previously.[9] To extend the comparison between the behavior of the three polymorphs, optimized-model-potential calculations have been made of the elastic constants of each.

Alloys in the In-Tl system crystallize in the fcc, bcc, and hcp, and the face-centred-tetragonal (fct) indium structure. Previously, elastic-constant measurements have been made on alloys belonging to the fct and fcc phases in the composition range 0- to 39-at.% Tl,[7,10,11] and it has been shown that the fcc-fct martensitic phase transition is accompanied by softening of the $\{110\}\langle1\bar{1}0\rangle$

acoustic-phonon mode close to the Brillouin-zone center.[12] The present work on the bcc alloys completes knowledge of the elastic constants of the In-Tl alloys by providing single-crystal data for the previously unstudied phase.

II. EXPERIMENTAL PROCEDURE

The Tl-rich end of the In-Tl phase diagram at atmospheric pressure relevant to the present work is illustrated in Fig. 1. The bcc and hcp solid solutions correspond to solutions of In in the β and ϵ polymorphs, respectively, of Tl. The bcc phase is arrested at the eutectoid, which according to Hansen and Anderko[13] has a composition of 75.6-at.% Tl and a temperature of 19 °C; more recent studies locate the eutectoid somewhat differently, see Meyerhoff and Smith[14]: 82.5-at.% Tl and 29.9 °C; Adler and Margolin[15]: 80.6-at.% Tl and -12.5 °C. Inspection of Fig. 1 reveals that the phase boundaries of the bcc phase determined by Adler and Margolin[15] are quite different from those of the other investigators.[13,14] The discrepancies may be due to the sluggish nature of the solid-state eutectoid reaction.[16] Strictly speaking it should not be possible to retain a bcc single-phase alloy below the eutectoid under equilibrium conditions. However, as part of a study of the superconducting transition temperatures T_c in the bcc phase of the In-Tl system, Luo and Willens[6] showed that the bcc phase can be retained at low temperatures by fast quenching. They found that alloys containing less than 60-at.% Tl or more than 83-at.% Tl were always two-phase and that only alloys with a composition between 75- and 83-at.% Tl stayed single-phase bcc after being kept at room temperature for a day. The alloys studied here fall in this composition range.

Large, homogenous single crystals suitable
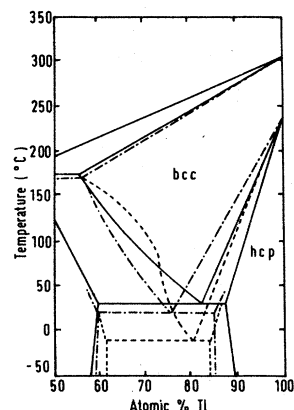
for ultrasonic-wave velocity measurements, of two compositions, 76.5- and 81.5-at.% Tl, were grown by a modified Bridgman method from previously well homogenized melts contained in a carbon-coated quartz tube sealed under a vacuum of better than 10^{-5} Torr. The cooling of the melt was accomplished by lowering the temperature profile in a vertical furnace at the rate of about 1 °C per hour by means of a preprogrammed ramp generator; the growth tube containing the melt was kept stationary. The starting materials—In ingot and Tl rod—were both 99.999% pure. The temperature gradient at the growth interface was about 30 °C cm^{-1}. After the growth process, the boules could be easily removed; there was no tendency to stick to the walls of the quartz tube. Etching the boules with 1 : 1 HNO$_3$ revealed grain boundaries. The grains were large enough to allow single crystal samples ($\sim 1.5 \times 1 \times 0.3$ cm^3) suitable for ultrasonic measurements to be readily obtained from them. The homogeneity of the alloys was ascertained by Debye-Scherrer powder photographs taken from different portions of the boule. The powder photographs revealed well-defined diffraction lines characteristic of a single-phase bcc structure; the lattice parameter was reproducible to within ±0.0005 Å along each boule. The measured lattice parameter (a) and the x-ray and floatation densities, respectively, were: for the 76.5-at.% Tl, 3.8312 ±0.0005 Å, 10.824 ±0.004 g cm^{-3} and 10.80 ±0.02 g cm^{-3}; for the 81.5-at.% Tl, 3.8345 ±0.0005 Å, 11.060 ±0.004 g cm^{-3} and 11.04 ±0.02 g cm^{-3}. The lattice parameters are in agreement with those reported by Luo and Willens[6] who estimated the actual compositions of their alloys to be within ±0.5% of the reported nominal compositions. Laue back-reflection photographs taken to orient the crystals in [110] and [100] directions to within ±$\frac{1}{2}$° revealed sharp undistorted spots characteristic of a strain-free single crystal. After orientation, samples for ultrasonic-wave velocity measurements were prepared by spark cutting and planing. The spark-planed sample end faces normal to [110] and [100] directions had a parallelism of better than 3×10^{-4} rad. X-cut longitudinal and Y-cut shear, quartz transducers of 6-mm diameter operated at their fundamental frequency (10 MHz) were used to generate and receive the ultrasound. Transducer bonding to the sample face was accomplished with "Nonaq" stop-cock grease. The pulse superposition method[17] was used to measure the ultrasonic-wave velocities. Low-temperature measurements were carried out in a standard cryostat with a temperature control of better than ±1 °K and the high temperature ones in a thermostatically controlled (±0.5 °C) oil bath. Further details of the experimental techniques can be found elsewhere.[18]

FIG. 1. The Tl-rich side of the In-Tl phase diagram. Dot-dash curve, Ref. 13; solid curve, Ref. 14; and dashed curve, Ref. 15.

TABLE I. Relationships between measured ultrasonic-wave velocities and elastic-stiffness constants.

Propagation direction	Polarization direction	Elastic-constant relationships	Ultrasonic-wave velocities v at 300°K (units: 10^5 cm sec^{-1})	
			In−76.5-at.%	In−81.5-at.% Tl
[100]	[100]	$\rho v_1^2 = C_{11}$	1.834	1.878
[100]	In (001) plane	$\rho v_2^2 = C_{44}$	0.947	0.957
[110]	[110]	$\rho v_3^2 = C_L = \frac{1}{2}(C_{11} + C_{12} + 2C_{44})$	2.02	2.051
[110]	[001]	$\rho v_4^2 = C_{44}$	0.946	0.952
[110]	[1$\bar{1}$0]	$\rho v_5^2 = C' = \frac{1}{2}(C_{11} - C_{12})$	0.399	0.434

III. ELASTIC BEHAVIOR OF THE bcc In-Tl ALLOYS

For a specified crystallographic direction, defined by direction cosines n_1, n_2, n_3, three bulk elastic waves can be propagated in a crystal with velocities v and the polarizations determined by the Christoffel equations

$$(L_{ik} - \rho v^2 \delta_{ik})u_{0k} = 0 \quad (i, k = 1, 2, 3). \tag{1}$$

Here u_{01}, u_{02}, u_{03} are the direction cosines of the particle displacement vectors and the L_{ik} are the Christoffel coefficients. For a cubic crystal there are three independent elastic constants C_{11}, C_{12}, and C_{44}. The eigenvalues and eigenvectors of the Christoffel equation for velocities of the modes which can be propagated in the [110] and [100]

directions of a cubic crystal are given in Table I. Although all the three elastic constants can be obtained from ultrasonic measurements in a [110] sample, agreement found with the results of [100] samples has proved a useful cross-check.

The temperature dependences of C_L, C_{44}, and C' of the 76.5 and 81.5 at% Tl alloys have been plotted in Figs. 2 and 3, respectively. In computing the temperature dependences of the elastic constants, corrections for sample length and density changes have been made using the thermal-expansion coefficient of 29×10^{-6} per °K for bcc alloys between 77 and 300 °K.[6] All the elastic constants show normal behavior with temperature: the temperature dependences of C_{ij} designated by the ratio $\Delta C_{ij}/C_{ij} = [C_{ij}(280 °K) - C_{ij}(320 °K)]/ C_{ij}(300 °K)$ are all positive, the values for the two alloys being: (i) In−76.5-at.% Tl, $\Delta C_L/C_L = 0.014$, $\Delta C_{44}/C_{44} = 0.043$, and $\Delta C'/C' = 0.058$; (ii)
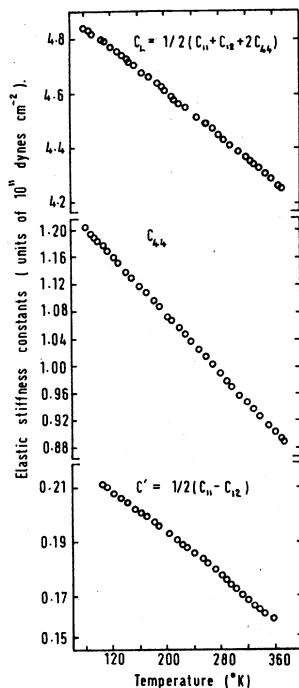
FIG. 2. Temperature dependences of the elastic constants of In−76.5-at.%-Tl alloy.
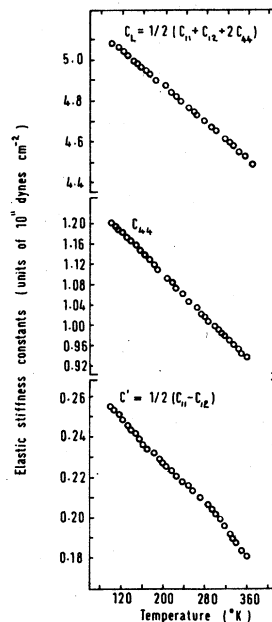
FIG. 3. Temperature dependences of the elastic constants of In−81.5-at.%-Tl alloy.

In–81.5-at.% Tl, $\Delta C_L/C_L = 0.019$, $\Delta C_{44}/C_{44} = 0.041$, and $\Delta C'/C' = 0.06$. The temperature variations of the elastic constants are remarkably linear and there are no discontinuities which would have arisen if the eutectoid reaction was taking place as the temperature was lowered. Irrespective of the rate of cooling ($\sim$0.75–2 °K min^{-1}), the ultrasonic wave velocities were all reproducible to three significant figures after a temperature run. Further evidence that the crystals did not change phase even after cooling down to as low as 80 °K was obtained from x-ray studies before and after each temperature run: Laue photographs established that after each cycle the single crystals had not altered and Debye-Scherrer powder photographs showed that the alloys retained the bcc single-phase structure. Apparently, there was not eutectoidal decomposition in these alloys at the rates of cooling employed. There is every reason to believe that the elastic constant data given in Figs. 2 and 3 correspond to those of single-phase bcc alloy crystals right down to 80 °K.

The elastic-stiffness constants C_{11}, C_{12}, and C_{44} and the compliance constants S_{11}, S_{12}, and S_{44} of the alloys have been calculated from the experimental results plotted in Figs. 2 and 3 and are given at selected temperatures in Table II. Each

elastic constant C_{ij} of the 81.5-at.% Tl alloy is stiffer at all the temperatures than the corresponding constant of the 76.5-at.% Tl alloy. This compositional dependence affects the value of C' much more than the other elastic constants. For example, at 300 °K for the 81.5-at.% Tl alloy, C' is 21% stiffer than that of the 76.5-at.% Tl alloy, whereas for C_{44} this difference is only 3.5%. Despite this increased stiffening, C' remains small compared to the other principal shear modulus C_{44}.

The elastic-constant results have been used to calculate the adiabatic compressibility β_s $[= -V^{-1}(\partial V/\partial P)_s = 3/(C_{11} + 2C_{12})]$; the values obtained are given in Table II at selected temperatures. β_s values at 300 °K for the different phase fields in the In-Tl alloy system have been plotted as a function of the composition in Fig. 4. Included in this plot are the isothermal compressibilities β_T $[= -V^{-1}(\partial V/\partial P)_T]$ for bcc alloys of comparable composition calculated from Bridgman's high-pressure data[19]; the difference $\beta_T - \beta_s$ is $TV\alpha^2/C_p$ and is approximately 0.7% only. Thus the present results for the compressibility of bcc alloys are in reasonable agreement with those of Bridgman.[19] The variation of the compressibility over the whole composition range from pure fct In through the

TABLE II. The elastic properties of bcc In-Tl alloys.

Composition (at.% Tl)	76.5			81.5		
Temperature (°K)	100	300	350	100	300	350
Elastic stiffness constants (in units of 10^{11} dyn cm^{-2})						
C_{11}	3.836	3.611	3.555	4.147	3.853	3.786
C_{12}	3.414	3.267	3.231	3.625	3.437	3.408
C_{44}	1.184	0.967	0.914	1.206	1.001	0.948
$C' = \frac{1}{2}(C_{11} - C_{12})$	0.211	0.172	0.162	0.261	0.208	0.189
Debye temperature (°K)						
Θ_D	79.6	72.2	70.2	82.9	75.3	72.5
Θ_l	200.7	192.5	190.5	204.5	195.8	193.5
Θ_{fs}	93.0	84.0	81.7	93.3	85.3	82.5
Θ_{ss}	60.2	54.6	53.1	63.4	57.4	55.1
Mean-square atomic displacement $\langle u^2 \rangle$ (Å^2)	0.038	0.135	0.168	0.034	0.121	0.153
Anisotropy factor $A = C_{44}/C'$	5.611	5.622	5.642	4.621	4.812	5.016
Elastic compliance constants (in units of 10^{-10} cm^{2}dyn^{-1})						
S_{11}	0.161	0.197	0.209	0.131	0.163	0.179
S_{12}	−0.076	−0.094	−0.099	−0.061	−0.077	−0.085
S_{44}	0.084	0.103	0.109	0.083	0.099	0.105
Bulk modulus B (in units of 10^{12} dyn cm^{-2}) $[= \frac{1}{3}(C_{11} + 2C_{12})]$	0.355	0.338	0.334	0.380	0.357	0.353
Compressibility β_S (in units of 10^{-12} cm^{2}dyn^{-1}) $(= B^{-1})$	2.81	2.96	2.99	2.63	2.80	2.83
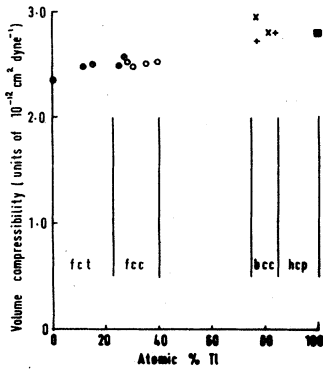
FIG. 4. Volume compressibilities of In-Tl alloys.
●, Ref. 11; o, Ref. 7; +; Ref. 19; and ■, Ref. 9.

FIG. 5. Anisotropy factor $A (= C_{44}/C')$ of bcc metals and alloys. Unless otherwise indicated the results are at 300 °K. Elastic-constant data have been obtained from Ref. 22 for Rb, Ref. 23 for Cs, and Ref. 24 for all the others.

fcc and bcc alloys to hcp Tl is surprisingly small: alloying between these two group-IIIB metals has only a small effect on the interatomic cohesive energy throughout the alloy system.

Resistance to shear of a cubic crystal is best characterized by the two moduli $C' = \frac{1}{2}(C_{11} - C_{12})$ and C_{44}. In these alloys the former modulus is much smaller than the latter and also exhibits stronger temperature dependence. Therefore, the anisotropy factor $A(=C_{44}/C')$ has large values and is sensitive to temperature and composition. Since the magnitude of C' in metallic bcc crystals relates to the occurrence of displacive phase transitions, the anisotropy factor A is a useful guide to the relative stability of these materials. The elastic behavior can be displayed with advantage on a plot of the reduced elastic stiffnesses C_{12}/C_{11} against C_{44}/C_{11}; here A can be represented by a fan of lines originating at the point ($C_{12}/C_{11} = 1$, $C_{44}/C_{11} = 0$), and the Cauchy relation $C_{12} = C_{44}$ for central-force crystals is a diagonal. The data for bcc metals and alloys plotted in this way (Fig. 5) can be compared with those for fcc materials collected together by Ledbetter and Moment.[20] The bcc metals and alloys separate into two distinct groups the members of which cluster into two different areas on this reduced elastic-stiffness diagram; the marked difference between stability of crystals in these two groups can be understood qualitatively on the basis of the elastic anisotropy of the shear moduli. (i) The bcc transition metals V, Cr, Nb, Mo, Ta, and W, which tend to be elastically isotropic, are rendered stable at all temperatures by long-range interactions between electrons in the unfilled d shells; the comparitively large magnitude of C' in these elements is related to the number of electrons per atom in the unfilled d bands.[21] (ii) The second group comprises those metals and alloys which crystallize in the bcc structure but transform to a close-packed structure on cooling. This latter
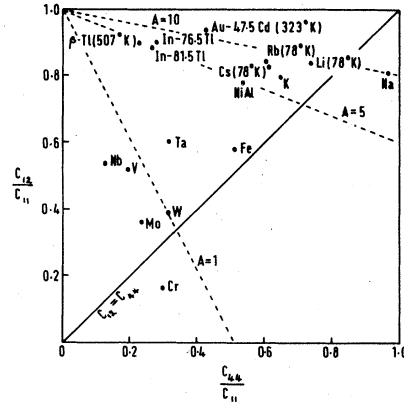
group, into which the bcc In-Tl alloys fall, includes the alkali metals and β brass. Zener[1,3] first pointed out that a bcc crystal comprised of rigid spheres (or of ions containing only closed shells) would show no resistance to a (110), [1$\bar{1}$0] shear and would tend to shear spontaneously on the (110) plane in a [1$\bar{1}$0] direction. He concluded that the corresponding shear modulus $\frac{1}{2}(C_{11} - C_{12})$ should be abnormally small in those bcc crystals in which the interatomic repulsive forces are qualitatively similar to those between contacting rigid spheres; such materials should be inherently mechanically unstable. For bcc Tl (ionic radius, 1.05 Å; a, 3.879 Å) like bcc Na (ionic radius, 0.98 Å; a, 4.225 Å), the ions are too small to overlap appreciably. The small values of $\frac{1}{2}(C_{11} - C_{12})$ found here for the bcc In-Tl alloys (Table II) conform to Zener's original prediction and establish that these alloys are not far from being mechanically unstable to a (110), [1$\bar{1}$0] shear. The large deviation from the Cauchy relation ($C_{12} = C_{44}$) shown in Fig. 5 indicates appreciable non-central-force contributions to the elastic constants.

The anisotropy of elastic behavior can be illustrated by polar plots of Young's modulus E. For a cubic crystal

$$1/E = S'_{11} = S_{11} - 2[(S_{11} - S_{12}) - \tfrac{1}{2}S_{44}](l_1^2 l_2^2 + l_2^2 l_3^2 + l_3^2 l_1^2),$$

(2)

where $l_i (i = 1, 2, 3)$ are the direction cosines of the applied stress direction. Thus when $A = 1$(i.e., $2(S_{11} - S_{12})/S_{44} = 1$), the condition for elastic isotropy, the polar plot is a sphere; the more A differs from unity, the more the cross sections deviate from circles. The (100) and (110) plane cross sections of the Young's modulus surface
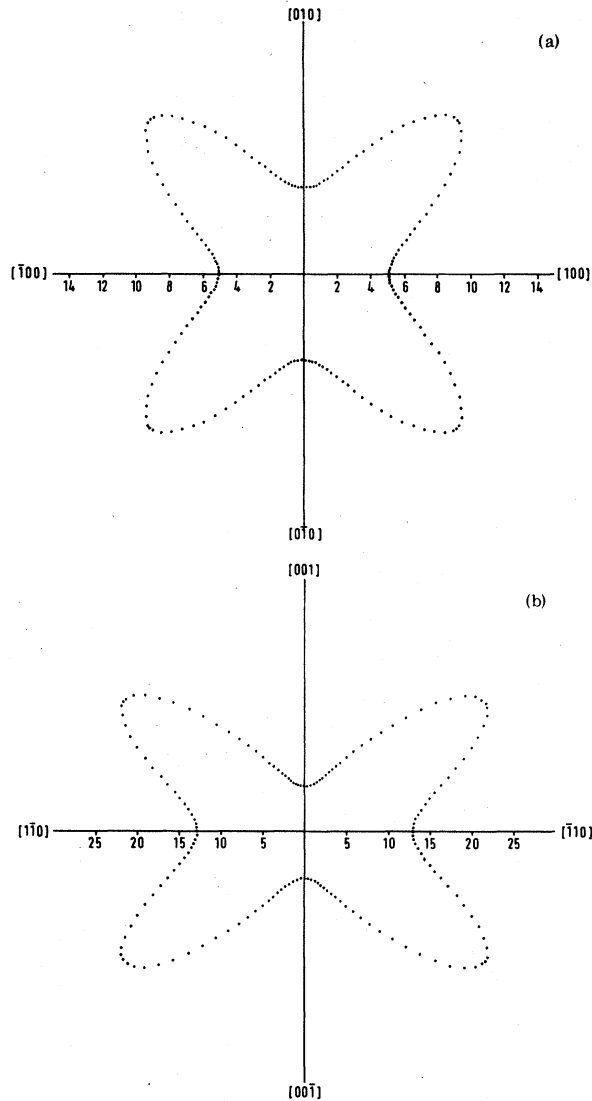
FIG. 6. The (a) (100) and (b) (110) plane cross sections of the Young's-modulus surface of In—76.5-at.% Tl at 300 °K. Units: 10^{10} dyne cm^{-2}.

FIG. 7. The (a) (100) and (b) (110) plane cross sections of the velocity surface of In—76.5-at.% Tl at 300 °K. Units: 10^{5} cm sec^{-1}.

shown in Fig. 6 for the In—76.5-at.%-Tl alloy at 300 °K emphasize the marked anisotropy of these alloys.

The Debye temperature Θ_D has been calculated from the ultrasonic-wave velocity measurements using the relation

$$\theta_D = \left(\frac{9N}{4\pi V}\right)^{1/3} \frac{h}{k} \Bigg/ \left[\int \left(\frac{1}{v_1^3} + \frac{1}{v_2^3} + \frac{1}{v_3^3}\right)\frac{d\Omega}{4\pi}\right]^{1/3}, \quad (3)$$

where N/V is the molar volume and v_i are the eigenvalues of the Christoffel equation (1). The integral over the solid angle has been approximated by a sum taken over 10 288 points each subtending an equal solid angle (= 1.218×10^{-3} Sr). To

obtain the velocities of the three modes which correspond to the propagation direction cosines n_1, n_2, n_3 the eigenvalues of the Christoffel equation (1) have been computed. (100) and (110) plane cross sections of the surfaces are shown in Fig. 7. The marked anisotropy of these velocity surfaces demonstrates the necessity for using a fine mesh grid of points in velocity space for the solution of the integral in Eq. (3) if an accurate Debye temperature is to be calculated. Using the elastic-constant-set obtained at a given temperature, one obtains $\theta_D(T)$ as distinct from Θ_0 the low-temperature limit. The calculated Debye temperatures are given in Table II. There is no specific-heat

TABLE III. Elastic properties of bcc β polymorph of Tl based on the alloy composition extrapolated elastic stiffnesses of bcc In-Tl alloys. The elastic constants at 507 and 577 °K are the temperature extrapolated values.

Temperature (°K)	100	300	350	507	577
Elastic stiffness constants (units: 10^{11} dyn cm^{-2})					
C_{11}	5.3	4.74	4.63	4.21	4.02
C_{12}	4.41	4.05	4.06	3.78	3.67
C_{44}	1.29	1.12	1.07	0.94	0.88
$C' = \frac{1}{2}(C_{11} - C_{12})$	0.44	0.34	0.28	0.21	0.17
Anisotropy ratio $A = C_{44}/C'$	2.93	3.29	3.82	4.48	5.18
Bulk modulus $B = \frac{1}{3}(C_{11} + 2C_{12})$ (units: 10^{12} dyn cm^{-2})	0.47	0.43	0.43	0.39	0.38
Compressibility $\beta_S = B^{-1}$ (units: 10^{-12} cm^2 dyn^{-1})	2.1	2.3	2.3	2.5	2.6
Debye temperature Θ_D (° K)	91.3	83.2	79.2	71.6	67.3

data for the bcc In-Tl alloys available at the present for comparison.

Debye temperatures for hcp Tl of 75 °K,[9] and 83.2 °K,[25] have been obtained from ultrasonic measurements made at 300 and 4.2 °K, respectively, and 85 °K from specific-heat data at low temperatures.[26] On the basis of these numbers, it is difficult to establish a precise value for the Debye temperature of hcp Tl. However, 80 ± 3 °K would seem to be an acceptable value for $\theta_D(T)$ for $T > \theta_D$.

Although a large number of metals exhibit polymorphism, elastic-constant data for different forms of the same metal are sparse. The elastic constants of the bcc form of Tl itself have been obtained by linear extrapolation of the bcc alloy data back to the pure-Tl limit. Results are presented in Table III. The elastic constants for all the polymorphs of Tl are compared in Table IV. The two cubic forms show very similar elastic behavior.

IV. OPTIMIZED-MODEL-POTENTIAL CALCULATIONS

Thallium is a nontransition element and for each of its polymorphs the ionic radii are small compared to the interionic distances; the small core approximation holds, and theoretical estimates of the lattice dynamics can be made for the fcc, bcc, and hcp forms using pseudopotential methods. To make such calculations, the real potential of each ion has been replaced by an optimized-model potential for Tl constructed following Shaw's modification[27] of the model potential[28] using the spectroscopic-term values of the free ion to determine the optimized-model parameters. The optimized-model parameters in atomic units evaluated at the estimated Fermi energy E_F (= -0.75 a.u.) were (in the nomenclature of Shaw): $A_0(E_F) = 1.38$, $A_1(E_F) = 1.63$, $A_2(E_F) = 1.10$, $(\partial A/\partial E)_{E_F} = -0.508$, $(\partial A_1/\partial E)_{E_F} = -0.468$, $(\partial A_2/\partial E)_{E_F} = -0.128$.[29] The screened form factor and the energy wave number

TABLE IV. The elastic-stiffness constants of the Tl polymorphs.

Elastic-stiffness constants (units: 10^{11} dyn cm^{-2})	$\subset$(hcp) Measured (300 K) (Ref. 9)	Theoretical	α(fcc) Extrapolated from exper. alloy data (300 K) (Ref. 8)	Theoretical	β(bcc) Extrapolated from exper. alloy data (300 K)	Theoretical
C_{11}	4.08	6.1	4.08	3.7	4.74	5.1
C_{12}	3.54	$\cdots$	3.40	3.0	4.05	3.7
C_{13}	2.9	$\cdots$	$\cdots$	$\cdots$	$\cdots$	$\cdots$
C_{33}	5.28	6.4	$\cdots$	$\cdots$	$\cdots$	$\cdots$
C_{44}	0.726	0.55	1.10	0.93	1.12	1.6
$\frac{1}{2}(C_{11} - C_{12})$	0.270	$\cdots$	0.34	0.35	0.34	0.7

characteristic $F(q)$ for Tl were then evaluated from a Fortran program based on a somewhat modified version of Shaw's original PL/I program. The effective valency $Z^*[= Z(1 - \rho)]$ can be taken as 3 for Tl so that the depletion hole ρ is zero. Using the local exchange-correlation potential,[28] exchange and correlation effects of the conduction electrons have been included. Knowledge of $F(q)$ allows calculation of the band-structure contribution to the energy of an electron in a state $|k\rangle$, that is $E_{bs}[=\sum_q' S^*(\vec{q})S(\vec{q})F(\vec{q})$, where the sum over $\vec{q}$ can readily be replaced by an integral].

The phonon dispersion curves have been calculated for the pure-mode directions for each of the three polymorphs; to expedite this, we first determine for a distortion of wave number $\vec{Q}$ the change δE_{tot} in the total energy

$$\delta E_{tot} = \delta E_{fe} + \delta E_{bs} + \delta E_{es} . \tag{4}$$

The change δE_{fe} in the free-electron energy is a second-order effect and can be neglected. For a crystal such as bcc or fcc containing only one atom per unit cell, the change δE_{bs} in the band-structure energy can be obtained using[30]:

$$\delta E_{bs} = \sum_{\vec{q}_0} [\,|(\vec{q}_0 + \vec{Q}) \cdot \vec{a}_{\vec{Q}}|^2 F(\vec{q}_0 + \vec{Q})$$
$$+ |(\vec{q}_0 - \vec{Q}) \cdot \vec{a}_{\vec{Q}}|^2 F(\vec{q}_0 - \vec{Q}) - 2|\vec{q}_0 \cdot \vec{a}_{\vec{Q}}|^2 F(\vec{q}_0)] . \tag{5}$$

where the $\vec{a}_{\vec{Q}}$ are normal coordinates representing propagating waves of wave number $\vec{Q}$ in the crystal and $\vec{q}_0$ is a lattice wave number. The change in the Ewald electrostatic energy of point ions in a uniform sea of negative charge for a single ion per unit cell for a distortion of wave number $\vec{Q}$ propagating along a pure-mode direction is given by[30]

$$\delta E_{es} = \frac{2\pi Z^{*2} e^2}{\Omega_0} \left[2|a_{\parallel}|^2 + \sum_{q_0}' \left(\frac{1}{(q_0^{\parallel} + \vec{Q})^2 + q_0^{\perp 2}} + \frac{1}{(q_0^{\parallel} - \vec{Q})^2 + q_0^{\perp 2}} \right. \right.$$
$$\left. \left. - \frac{2}{q_0^{\parallel 2} + q_0^{\perp 2}} \right)(|\vec{q}_0^{\perp} \cdot \vec{a}_{\perp}|^2 - q_0^{\perp 2}|a_{\parallel}|^2 \right] . \tag{6}$$

Here $q_0^{\parallel}$ and $\vec{q}_0^{\perp}$ are the components of $\vec{q}_0$ parallel and perpendicular to $\vec{Q}$; similarly $a_{\parallel}$ and $a_{\perp}$ are the components of $\vec{a}$.

Using Eqs. (5) and (6), δE_{bs} and δE_{es} have been obtained for the three displacement vectors corresponding to one longitudinal and two transverse waves propagated along the [001] and [110] directions in bcc and fcc Tl. Then the potential energy change per ion due to the distortion can be obtained as

$$\delta E_{bs} + \delta E_{es} = \sum_{i=1,3} E_i \vec{a}_i^2 . \tag{7}$$

For an ion of mass M the kinetic energy per ion is $M\sum_{i=1,3} \vec{a}_i^2$ and the frequencies for the given distortion can be obtained from

$$\omega_i^2 = E_i/M . \tag{8}$$

The propagation velocity of an ultrasonic wave can then be found from the slope $\partial\omega/\partial\vec{Q}$ close to the Brillouin zone center $\vec{Q} = 0$ and thus the elastic-stiffness constants from $\rho v^2 = C_{ij}$. The elastic constants calculated in this way for the bcc and fcc modifications of Tl are compared with the "experimental" values, (i.e., extrapolated from alloy data) in Table IV. The changes in the electrostatic and band-structure energies have an opposite sign; from this cancellation between these two contributing terms to δE_{tot} and thus eventually to the calculated elastic constants derives a major source of inaccuracy. In terms of the overall accuracy expected of lattice dynamical calculations by pseudopotential methods, the agreement between the calculated and "experimental" values is acceptable and provides some basis for confidence in the extrapolation procedure used to find "experimental" values of the bcc and fcc polymorphs of Tl. The phonon dispersion curves for $\vec{Q}$ along the T, Σ, and Δ directions in the wave-number lattice were computed for hcp Tl by calculating δE_{bs} and δE_{es} following the methods described by Harrison[30] and extended by Pindor and Pynn.[31] C_{11}, C_{33}, and C_{44} have been calculated from $(\partial\omega/\partial\vec{Q})_{\vec{Q}\to 0}$ and results are given in Table IV. Since the lattice dynamical calculations have been made only for pure-mode directions, C_{13} has not been obtained because this tensor component only occurs (in combination with other moduli) for wave propagation along directions which are not pure. A more important feature is that $\frac{1}{2}(C_{11} - C_{12})$ is very sensitive to variations of the input model parameters for Tl including the Fermi level E_F; in fact, the corresponding calculated phonon dispersion curve (in the Σ direction) can be made to take a negative value near the zone center, corresponding to a negative $\frac{1}{2}(C_{11} - C_{12})$, which would violate a Born stability criterion. This finding emphasises the incipient instability of hcp Tl.

V. HIGH-TEMPERATURE STABILITY OF bcc Tl

The existence of the bcc to hcp structural transformation in Tl requires that the Gibbs free energy $G(T, P)$ (equal to $U + PV - TS$) curves for the two phases intersect. Thus the stability of the phases is determined by two factors: (i) the binding energy at absolute zero and (ii) the entropy. The internal energy of close-packed structures should be lower than that of the bcc structure and hence the close-packed structure is expected to be stable at low temperatures.[1-3] However, in general, the looser the packing of a structure , the greater will be the entropy of vibration. Due to the abnormally small value of $\frac{1}{2}(C_{11} - C_{12})$, as the temperature is raised, there is a large amplitude of vibration of the (110), $[1\bar{1}0]$ shear strain coordinate; this produces a large vibrational entropy contribution and thus a more rapid decrease of free energy with temperature for the bcc than for the close-packed structures. Thus the bcc structure is thermodynamically favored at high temperatures. Zener's old argument has recently been examined by detailed analysis by Grimvall and Ebbsjö[4] who point out that there are no measurements of elastic constants or of neutron or x-ray scattering experiments that can be used to put the idea to a firm experimental test.

The present experimental results can be used to examine the hypothesis that the stability of the bcc structure at high temperatures is due to its larger vibrational entropy. In the first place, of course, the finding that $\frac{1}{2}(C_{11} - C_{12})$ is small in the bcc alloys provides direct confirmatory evidence. Previously, measurements of the latent heats of phase transition between the low-temperature close-packed and the bcc phases have shown that the excess entropy of the bcc phase is equivalent to a sizable proportion of the entropy of melting. In the harmonic approximation, the free energy of phonons having a frequency spectrum $f(\nu)$ is given by

$$G_{\text{ph}} = kT \int \ln\left[2\sinh\left(\frac{h\nu}{2kT}\right)\right] f(\nu)\, d\nu. \tag{9}$$

Grimvall and Ebbsjö[4] proceed by defining a characteristic temperature that corresponds to a geometrical average of the phonon frequencies and find that at high temperatures where T is greater than Θ,

$$G_{\text{ph}} \sim 3NkT \ln(\Theta/T), \tag{10}$$

where N is the number of atoms.

In general the difference $\Delta\Theta$ $[= (\Theta_1 - \Theta_2)]$ between the characteristic temperatures of the two polymorphs will be small and to a reasonable approximation the phonon spectrum can be replaced either by the Einstein or Debye model. Then the Helmholtz free energy and entropy at a temperature T can be written as:

Einstein model.

$$F = \Phi_0 + \tfrac{3}{2}Nk\Theta_E + 3NkT \ln(1 - e^{-\Theta_E/T}), \tag{11}$$

$$S = -\left(\frac{\partial F}{\partial T}\right)_V = 3Nk[(\Theta_E/T)(e^{\Theta_E/T} - 1)^{-1} - \ln(1 - e^{-\Theta_E/T})]; \tag{12}$$

Debye model.

$$F = \Phi_0 + 9N\left[\tfrac{1}{8}k\Theta_D + kT\left(\frac{T}{\Theta_D}\right)^3 \int_0^{\Theta_D/T} \zeta^2 \ln(1 - e^{-\zeta})\, d\zeta\right], \tag{13}$$

$$S = 3Nk\left[-\ln(1 - e^{-\Theta_D/T}) + 4\left(\frac{T}{\Theta_D}\right)^3 \int_0^{\Theta_D/T} \frac{\zeta^3}{e^\zeta - 1}\, d\zeta\right], \tag{14}$$

where Φ_0 is the static crystal potential and the other notations take their usual significance.[32] It can be shown that the excess entropy S of the bcc (β) phase over that of the hcp(ϵ) phase when $T > \Theta$ is given for the Einstein model by

$$\Delta S = S^\beta - S^\epsilon = 3Nk \ln(\Theta_E^\epsilon/\Theta_E^\beta), \tag{15}$$

and for the Debye model of vibration spectrum by

$$\Delta S \simeq 3Nk \ln(\Theta_D^\epsilon/\Theta_D^\beta). \tag{16}$$

From these expressions it is possible to calculate the excess entropy and the difference $-T(S^\beta - S^\epsilon)$ in the vibrational entropy contribution to the free energy between the two polymorphs once the Debye or the Einstein temperatures are known.

Using 71.6 °K (Table III) and 80 ± 3 °K for Θ_D(507 °K) of bcc and hcp Tl, respectively, the excess entropy of the bcc structure calculated using Eq. (16) is $(0.35 \pm 0.15)k$ per atom. The value obtained from latent heat ($T\Delta S$) measurements was $(0.18 \pm 0.02)k$ per atom.[33]

Friedel[33] has suggested that the high-temperature stability of the bcc phase may be related to the fact that it is an *alternate* structure (i.e., a closed circuit of interatomic jumps between successive nearest neighbors requires an even number of jumps) while the hcp and fcc structures are not. The expression found by Friedel for the excess entropy of the bcc phase (β) over the hcp phase (ϵ), written in the same terminology used here for Eqs. (15) and (16), is for the Einstein model

$$\Delta S = S^\beta - S^\epsilon \simeq 3Nk \{\ln(\omega_E^\epsilon/\omega_E^\beta)$$
$$- \hbar^2/24k^2T^2[(\omega_E^\beta)^2 - (\omega_E^\epsilon)^2]\} \tag{17}$$

(where ω_E is the Einstein frequency) or in terms

of the number of nearest neighbors p

$$\Delta S \simeq 3Nk[\tfrac{1}{2}\ln(p^\epsilon/p^\beta) - (p^\beta - p^\epsilon)(\hbar\omega_E^\epsilon)^2/24p^\epsilon k^2 T^2].$$

$$(18)$$

The Einstein temperature Θ_E is approximately $\tfrac{3}{4}\Theta_D$ (and so is ~54 °K for bcc Tl and ~60 °K for hcp Tl). For $T > \Theta_E$ which is true at the polymorphic transition temperature 507 °K, the second term in Eq. (18) is negligible (it is 0.002% of the first term). The excess entropy of the bcc phase is then

$$\Delta S \simeq \tfrac{3}{2}Nk\ln(12/8) = 0.6Nk.$$

$$(19)$$

Thus in the case of the bcc to hcp transformation in Tl the excess entropy calculated on the basis of number of nearest neighbors and the consequent reduction in the Einstein frequency of the more open bcc structure is three times greater than that obtained from latent-heat measurements and

twice that obtained from the elastic-constant data. The discrepancy may arise from a strong contribution to the elastic constants from the higher-order neighbors which the Friedel model does not take into account.

It can be concluded that in agreement with Zener's predictions (i) the shear stiffness constant $\tfrac{1}{2}(C_{11} - C_{12})$ of bcc In-Tl alloys is small and (ii) the stability of the bcc phase at high temperatures is due to the lower Debye temperature and excess vibrational entropy relative to the hcp structure.

ACKNOWLEDGMENTS

[1]C. Zener, *Elasticity and Anelasticity of Metals* (University of Chicago, Chicago, 1948).

[2]C. Zener, *Phase Stability in Metals and Alloys,* edited by P. S. Rudman, J. Stringer, and R. I. Jaffee (McGraw-Hill, New York, 1967).

[3]C. Zener, Phys. Rev. 71, 846 (1947).

[4]G. Grimvall and I. Ebbsjö, Phys. Scr. 12, 168 (1975).

[5]P. N. Adler and H. Margolin, Trans. Metall. Soc. AIME 230, 1048 (1964).

[6]H. L. Luo and R. H. Willens, Phys. Rev. 154, 436 (1967).

[7]D. B. Novotny and J. F. Smith, Acta Metall. 13, 881 (1965).

[8]M. L. Shepard and J. F. Smith, Acta. Metall. 15, 357 (1967).

[9]R. W. Ferris, M. L. Shepard, and J. F. Smith, J. Appl. Phys. 34, 768 (1963).

[10]N. G. Pace and G. A. Saunders, Proc. R. Soc. A 326, 521 (1972).

[11]D. J. Gunton and G. A. Saunders, Solid State Commun. 14, 865 (1974).

[12]D. J. Gunton and G. A. Saunders, Solid State Commun. 12, 569 (1973).

[13]M. Hansen and K. Anderko, *Constitution of Binary Alloys* (McGraw-Hill, New York, 1958).

[14]R. W. Meyerhoff and J. F. Smith, Acta Metall. 11, 529 (1963).

[15]P. N. Adler and H. Margolin, Acta Metall. 14, 1645 (1966).

[16]F. N. Rhines, *Phase Diagrams in Metallurgy* (McGraw-Hill, New York, 1956).

[17]H. J. McSkimin, J. Acoust. Soc. Am. 33, 12 (1961).

[18]R. I. Cottam and G. A. Saunders, J. Phys. C 6, 2105 (1973).

[19]P. W. Bridgman, Proc. Am. Acad. Arts Sci. 84, 1 (1955).

[20]H. M. Ledbetter and R. L. Moment, Acta Metall. 24, 891 (1976).

[21]E. S. Fisher and D. Dever, Acta Metall. 18, 265 (1970).

[22]E. J. Gutman and J. Trivisonno, J. Phys. Chem. Solids 28, 805 (1967).

[23]F. J. Kollarits and J. Trivisonno, J. Phys. Chem. Solids 29, 2133 (1968).

[24]L. K. France, C. S. Hartley, and C. N. Reid, Met. Sci. J. 1, 65 (1967).

[25]R. B. Weil, Ph.D. thesis, (University of California, Riverside, California, 1965) (unpublished).

[26]B. J. C. van der Hoven and P. H. Keesom, Phys. Rev. A 135, 631 (1964).

[27]R. W. Shaw, Phys. Rev. 174, 769 (1968).

[28]V. Heine and I. V. Abarenkov, Philos. Mag. 9, 451 (1964).

[29]D. J. Gunton, Ph.D. thesis (University of Durham, Durham, England, 1973) (unpublished).

[30]W. A. Harrison, *Pseudopotentials in the Theory of Metals* (Benjamin, New York, 1966).

[31]A. J. Pindor and R. Pynn, J. Phys. C 2, 1037 (1969).

[32]D. C. Wallace, *Thermodynamics of Crystals* (Wiley, New York, 1972).

[33]J. Friedel, J. Phys. (Paris) 35, L59 (1974).